

12-29-1993

Calcium Phosphate in Aspergillosis of the Maxillary Sinus

Hidekuni Tanaka

Nihon University School of Dentistry at Matsudo

Toshiro Sakae

Nihon University School of Dentistry at Matsudo

Hiroyuki Mishima

Nihon University School of Dentistry at Matsudo

Hirotsugu Yamamoto

Nihon University School of Dentistry at Matsudo

Follow this and additional works at: <https://digitalcommons.usu.edu/microscopy>

 Part of the [Biology Commons](#)

Recommended Citation

Tanaka, Hidekuni; Sakae, Toshiro; Mishima, Hiroyuki; and Yamamoto, Hirotsugu (1993) "Calcium Phosphate in Aspergillosis of the Maxillary Sinus," *Scanning Microscopy*. Vol. 7 : No. 4 , Article 13. Available at: <https://digitalcommons.usu.edu/microscopy/vol7/iss4/13>

This Article is brought to you for free and open access by the Western Dairy Center at DigitalCommons@USU. It has been accepted for inclusion in Scanning Microscopy by an authorized administrator of DigitalCommons@USU. For more information, please contact digitalcommons@usu.edu.

CALCIUM PHOSPHATE IN ASPERGILLOSIS OF THE MAXILLARY SINUS

Hidekuni Tanaka*, Toshiro Sakae¹, Hiroyuki Mishima¹ and Hirotsugu Yamamoto

Departments of Oral Pathology and ¹Anatomy, Nihon University School of Dentistry at Matsudo,
Chiba 271, Japan

(Received for publication October 23, 1993, and in revised form December 29, 1993)

Abstract

The unique appearance of apatite in fungus balls of aspergillosis in the maxillary sinus was investigated using scanning electron microscopy (SEM), energy-dispersive spectroscopy (EDS), X-ray microdiffraction and Fourier transform infrared spectroscopy (FT-IR). Rod-shaped fragments with tubular structures, and globular vesicles covered with conidia were observed in the fungus balls. Massive fragments of a solid substance were demonstrated inside the fungus balls. Calcium and phosphate were detected in necrotic areas of the fungus balls by EDS. X-ray microdiffraction and FT-IR showed the presence of an apatite-like substance, but failed to demonstrate the presence of calcium oxalate crystals usually found in such fungus balls.

Key Words: Aspergillosis, maxillary sinusitis, calcium phosphate, scanning electron microscopy, energy-dispersive spectroscopy, X-ray microdiffraction, Fourier transform infrared spectroscopy.

Introduction

Recently, reports of fungal infection of the paranasal sinus have increased, mainly in the otorhinolaryngology literature [1, 17] and to a lesser extent in the oral surgery literature [18, 19]. The necrotic calcified material has been reported to be calcium oxalate [3, 4, 10, 14]. Deposition of calcium oxalate is considered to be a consequence of metabolic activity in aspergillosis, and no other crystalline phase has been associated with the disease [3].

This paper presents a case of aspergillosis of the maxillary sinus involving calcium phosphate formation, a new finding as far as the authors are aware.

Materials and Methods

Materials

The materials used in this study were removed from the right maxillary sinus of a 53-year-old Japanese woman. She had undergone extraction of the upper right first molar in September 1988, following which the extraction cavity perforated through to the right sinus. Thereafter, she complained of spontaneous pain and swelling in the right buccal region, and subsequently visited our hospital in May 1989. On her first visit, laboratory tests and examination of her general condition showed no abnormalities. A diffuse radiopaque lesion was found upon radiological examination (Fig. 1). She was diagnosed clinically as having odontogenic maxillary sinusitis, and removal of the lesion was carried out in June 1989. Macroscopically, the removed materials consisted of grayish rubbery edematous sinus mucosae with partial necrotic bleeding and some calcified materials (Fig. 2).

Light microscopy

Following fixation with 10% neutral formaldehyde solution, the materials were cut into several pieces and routine paraffin sections were made. The sections were stained with hematoxylin and eosin as well as by various other staining techniques including the periodic acid-Schiff reaction, Grocott-methenamine-silver (GMS) and von Kossa's method, in order to search for fungal

*Address for correspondence:
Hidekuni Tanaka,
Department of Oral Pathology,
Nihon University School of Dentistry at Matsudo,
2-870-1 Sakaecho-Nishi,
Matsudo, Chiba, 271,
Japan

Telephone Number: 81-473-68-6111 Ext. 385
FAX Number: 81-473-64-6295

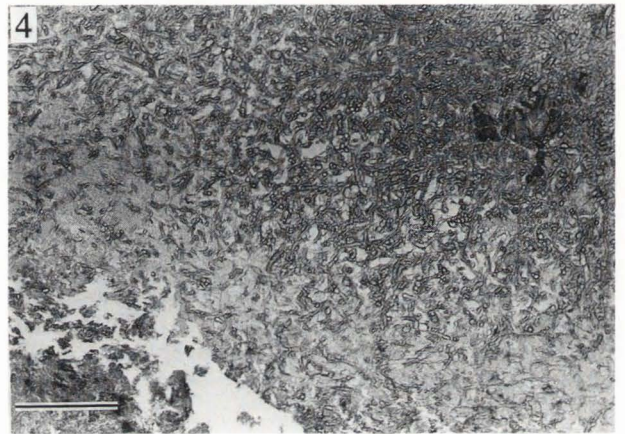
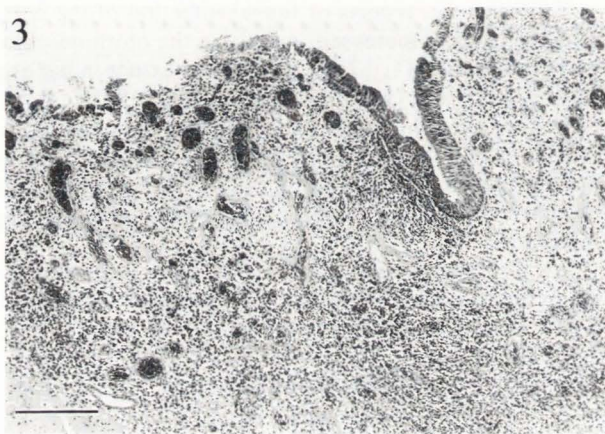
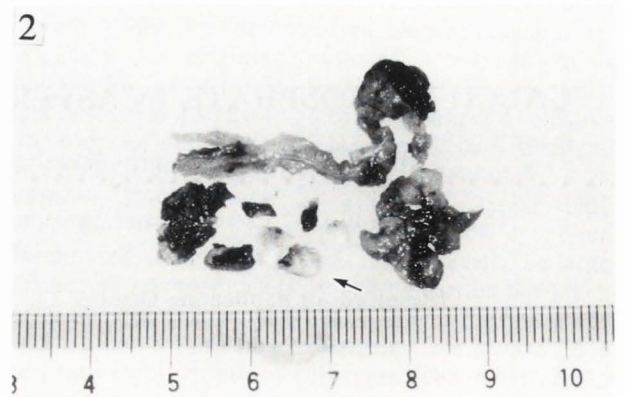
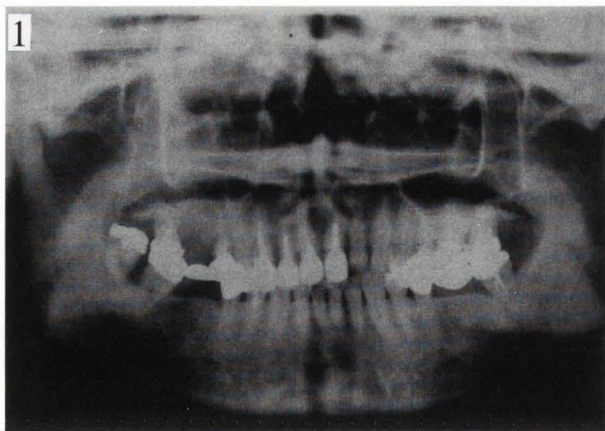


Figure 1. Panoramic radiograph showing a diffused radiopaque in the right maxillary sinus.

Figure 2. Macroscopical view of sinus revealing inflammatory mucosae with partially necrotic areas (arrow).

Figure 3. Photomicrograph of several infiltrating round cells and capillary dilatation covering with rough cuboidal and ciliated columnar epithelia (HE). Bar = 200 μm .

Figure 4. Microscopic view of a mass of fungal hyphae with the characteristic appearance of aspergillus (GMS). Bar = 100 μm .

hyphae. These specimens were observed by light and polarizing microscopy.

Electron microscopy

Part of the material fixed with 10% neutral formaldehyde solution was washed with distilled water (DW) and refixed with 2% glutaraldehyde and 1% osmium tetroxide. The material was washed with DW, dehydrated in a graded ethanol series, substituted with isoamyl acetate, and subjected to critical-point drying with carbon dioxide. After being sputter-coated with gold, the material was examined with a JEOL T-200 scanning electron microscope (SEM).

Energy-dispersive spectroscopy (EDS)

Part of the material fixed with 10% neutral formaldehyde solution was washed with DW, dehydrated in a graded ethanol series, substituted with isoamyl acetate,

and subjected to critical-point drying with carbon dioxide. The surface of the material was not polished. EDS analysis was carried out by point-mode analysis on carbon-coated samples using a JEOL JED-2000 attached to the JEOL T-200 SEM under the following measurement conditions: accelerating voltage, 25 kV; working distance, 20 mm; X-tilt angle, 30°; take-off angle, 41.18°; counting time, 100 seconds. The atomic percentages of the elements were calculated using an AUTO-ZAP program assuming the total percentage weight of cationic atoms to be 100.

X-ray microdiffraction

X-ray microdiffraction patterns of powder samples were obtained using an X-ray microdiffractometer (Rigaku, Tokyo) under the following conditions: X-ray tube voltage, 40 kV; tube current, 20 mA; target, Cu;

filter, Ni (wavelength, 0.15418 nm); scan speed, 1 degree (2θ)/min; time constant, 2.

Fourier transform infrared spectroscopy (FT-IR)

FT-IR was performed on KBr pellets using a Perkin-Elmer model 1600 spectrometer.

Results

Microscopically, histological examination showed severe inflammatory cell infiltration, fibrosis, capillary dilatation and edema in the submucosa covered with rough cuboidal and ciliated columnar epithelia (Fig. 3). Fungus balls were found in the lumen of the sinus with partially calcified necrotic areas. The fungi were composed of a mass of fungal hyphae and/or conidiophores, which branched in a peculiar unidirectional orientation, using GMS staining which revealed the characteristic appearance of *Aspergillus* (Fig. 4). Calcified material was assumed to be stained black by von Kóssa's method. Under polarizing microscopy, weak birefringence was observed in the necrotic areas of the fungus balls, but no strong birefringence such as that shown by calcium oxalate was evident.

Under SEM, the fungus balls showed rod-shaped fragments which corresponded to conidiophores and/or hyphae, and a globular formation that was considered to be a vesicle. Sterigmata and granulated conidial heads were found on the surface of the vesicle. The conidiophores or hyphae showed a Y-shaped three-dimensional pattern (Fig. 5). These fungal structures were not seen inside the fungus balls, but massive solid substances were observed (Figs. 6 and 7). Figure 6 shows the appearance of the rough surface of the glass-like amorphous materials.

The results of EDS analysis of fungus balls are given in Fig. 8 and Table 1. Calcium and phosphate were identified as the main components in necrotic areas of the fungus balls. The average Ca/P molar ratio of the analyzed material was 1.78 ± 0.12 ($n = 10$).

X-ray microdiffraction patterns were obtained from the fungus balls, and the diffraction patterns of the material was compared with the data in a previous report [9]. The X-ray microdiffraction patterns of fungus balls had features similar to those of low-crystalline, so-called, biological apatite: superimposed on a broad amorphous background, peaks occurred at 25.8° and $31-33^\circ 2\theta$ s, the location of the major apatite peaks (Fig. 9).

The FT-IR spectrum of the fungus balls is shown in Figure 10. The strong absorption bands at 565, 603, 872, 962, 1041, 1455, 1507, 1656 and 2926 cm^{-1} were comparable to those of hydroxyapatite (HAP), which occur at 563, 601, 872, 961, 1031 and 2963 cm^{-1} . The absorption bands at 565, 603, 872, 962 cm^{-1} corresponded to phosphate, and those at 1500 to 1600 cm^{-1} are due to protein components [8].

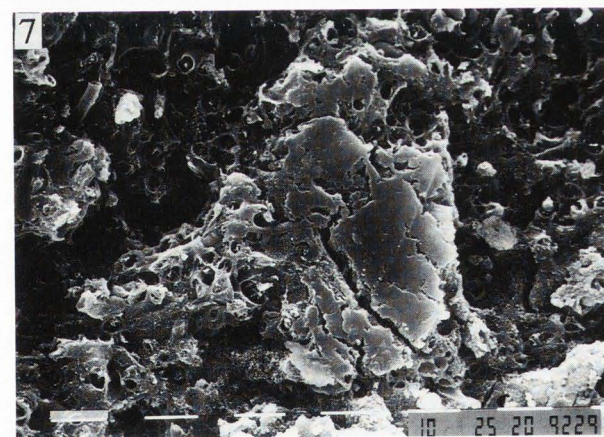
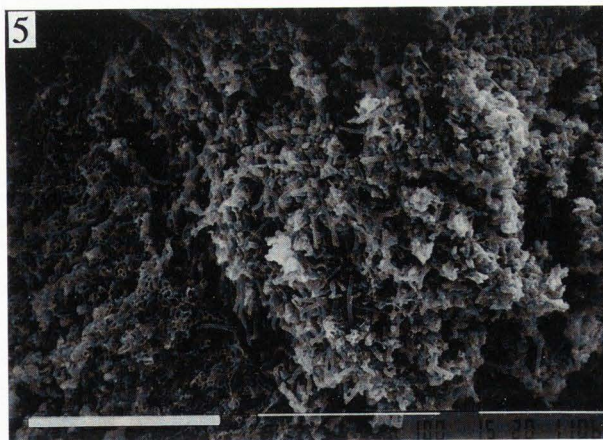


Figure 5. Scanning electron micrograph on surface of the fungus ball showing conidiophore and vesicle. Bar = $100\ \mu\text{m}$.

Figure 6. Scanning electron micrograph revealing the massive fragments solid substance inside of the fungus balls. Bar = $10\ \mu\text{m}$.

Figure 7. Scanning electron micrograph inside of the fungus balls. Bar = $10\ \mu\text{m}$.

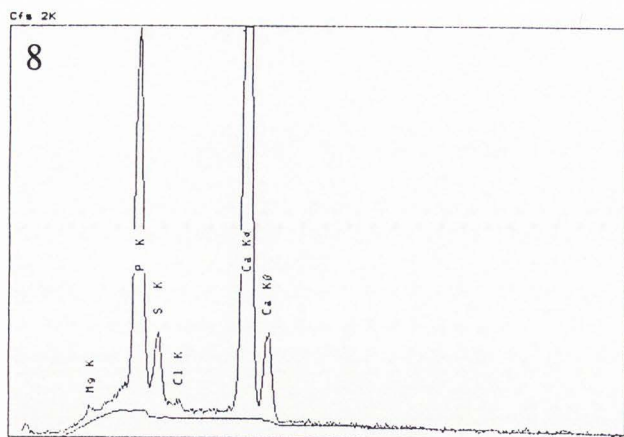


Figure 8. EDS data of fungus balls.

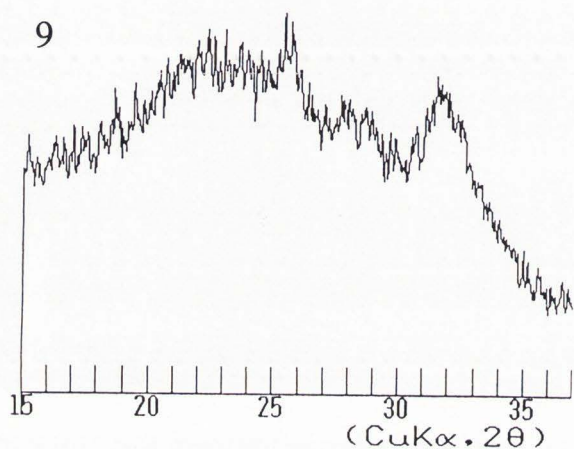
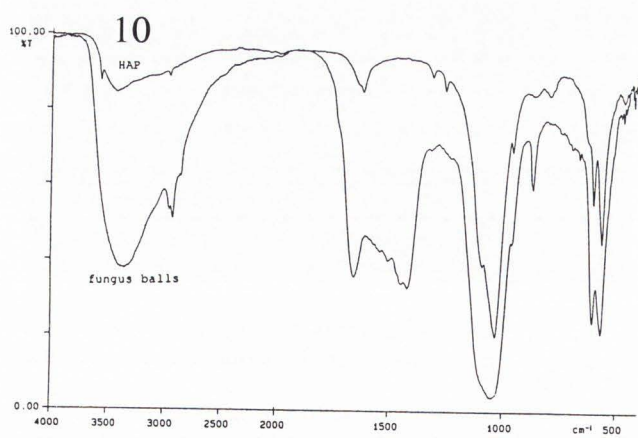


Figure 9. X-ray microdiffraction pattern of fungus balls.



HAP (cm⁻¹)	2963	-	-	-	1031	961	872	601	563
fungus balls (cm⁻¹)	2926	1656	1507	1455	1041	962	872	603	565

Figure 10. FT-IR pattern of fungus balls.

Table 1. EDS analysis data for fungus balls.

Element	Line	Weight %	Normalized atomic %	Net intensity
Mg	K	2.08	3.08	8.43
P	K	26.84	31.19	244.25
S	K	7.64	8.58	55.09
Cl	K	1.61	1.64	12.07
Ca	K	61.82	55.52	319.03
Total		100.00	100.00	

Discussion

Morphologically, the septate vegetative hyphae of *Aspergillus* grow in or over the substrate. At intervals, the cell branches and sends a fertile hypha or conidiophore into the air; the top of the conidiophore enlarges to form a vesicle, upon which numerous sterigmata are attached radially [2, 6, 15]. Mature sterigmata with their simple or branched secondary segments are approximately 15 mm long [20]. Generally, in aerobic conditions, the conidiophore (fruiting body or conidial head) may be well developed [6]. However, these structures were not seen inside the fungus balls, since the environment was anaerobic. This observation was in agreement with a SEM study reported by Hibino and Mori [5].

The necrotic areas of the fungus balls were investigated using von Kóssa's staining and EDS analysis to show their chemical components. SEM observation was performed to search for structural differences in the fungus. In the present study, calcium phosphate was found mainly surrounding the necrotic areas by von Kóssa's staining. Under polarizing microscopy, strong birefringence characteristic of calcium oxalate was not observed in these regions. EDS analysis showed that calcium and phosphate were present in these regions. The average Ca/P molar ratio was 1.78 ± 0.12 . The results of X-ray microdiffraction indicated the presence of an apatite-like substance, and the FT-IR absorption bands were in good agreement with data for HAP, although with infrared absorption analysis, it may be difficult to distinguish apatite from whitlockite. Based on the data summarized above, apatite was the main deposit in the calcified foci in the fungus balls. The deposition of apatite in aspergillosis has not been reported previously.

Nime and Hutchins [14] studied 68 patients with aspergillosis from autopsy and surgical pathology files, and reported that eleven had calcium oxalate deposition in areas affected by aspergillosis using histochemistry only. Among these eleven patients, six had sinusitis with fungus balls in the antrum. Hara *et al.* [4] also detected calcium oxalate monohydrate in fungal infection using X-ray diffraction, histochemistry and polarizing microscopy. Deposition of calcium oxalate may be a consequence of metabolic activity in aspergillosis [3, 10].

Biological apatites are the main mineral constituents of vertebrates bones and teeth. Pathological mineral deposits such as dental calculus, bursitis, arthritis and various other forms of ectopic calcification also include apatite-like materials [9, 11, 16]. The process of calcium phosphate mineralization, where biologically active molecules may behave as both inhibitors and promoters of crystal growth, opens up intriguing possibilities for explaining the exquisite control observed during biomineralization [7, 13]. A number of minerals of biological importance can precipitate as different phases and polymorphs depending on pH conditions, supersaturation, ionic strength, temperature and the nature of the solid phases already present. Nancollas and Gaur [12] reported that depending on the relative supersaturation, and the presence of natural inhibitors, both calcium oxalate and calcium phosphate phases may form in solution after the addition of calcium oxalate seed crystals.

The present study revealed that the calcified material deposited in a case of aspergillosis was biological apatite. The cause of deposition of biological apatite is obscure, but there are several possible reasons, including nucleation of calcium phosphate on calcium oxalate seed crystals, conversion of calcium oxalate into calcium phosphate, or direct precipitation of calcium phosphates due to excessive phosphate production by the metabolic activity of *Aspergillus*.

Acknowledgments

The authors thank Mr. M. Isozaki and Ms. S. Niimi, Perkin-Elmer Japan Co., Ltd, for use of FT-IR. This research was supported by a Grant-in-Aid for Scientific Research from the Ministry of Education, Science and Culture, Japan (Subject No. 04857218).

References

1. Chakrabarti A, Sharma SC, Chandler J (1992). Epidemiology and pathogenesis of paranasal sinus mycoses. *Otolaryng Head Neck Surg* **107**: 745-750.
2. Chandler FW, Kaplan WK, Ajello LA (1980). *A Color Atlas and Textbook of the Histopathology of Mycotic Disease*. Wolfe, London. pp. 34-37.
3. Hara M, Ikeda D, Isahaya S, Naoe S (1977). Aspergilloma by *Aspergillus niger* with calcium oxalate deposition report of autopsy. *Jpn J Med Mycol* **18**: 102-107 (in Japanese).
4. Hara M, Misugi K, Shimanouchi H (1976). Aspergilloma by *Aspergillus niger* with calcium oxalate deposition. Histochemical and X-ray diffraction study. *Yokohama Med Bull* **27**: 115-121.
5. Hibino J, Mori T (1985). Studies on treatment of tracheobronchopulmonary aspergillosis. Clinical, pathological and electron microscopic studies. *Jpn J Med Mycol* **26**: 300-309 (in Japanese).
6. Iwata K (1981). Pathogenic Microbiology. Nanzando, Tokyo. pp. 493-529 (in Japanese).
7. Johnsson MS, Nancollas GH (1992). The role of brushite and octacalcium phosphate in apatite formation. *Crit Rev Oral Biol* **3**: 61-82.
8. Keller RJ (1986). *The Sigma Library of FT-IR Spectra* (edition 1). Sigma Chemical, St. Louis. pp. 541-568.
9. LeGeros RZ, LeGeros JP (1984). Phosphate minerals in human tissues. In: *Phosphate Minerals*. Nriagu JO, Moore PB (eds.). Springer-Verlag, New York. pp. 351-385.
10. Metzger JB, Garagusi VF, Kerwin DM (1984). Pulmonary oxalosis caused by *aspergillus niger*. *Am Rev Res Dis* **129**: 501-502.
11. Nancollas GH (1982). Phase transformation during precipitation of calcium salts. In: *Biological Mineralization and Demineralization*. Nancollas GH (ed.). Springer-Verlag, New York. pp. 79-99.
12. Nancollas GH, Gaur SS (1984). Crystallization in urine. *Scanning Electron Microsc* **1984**;IV: 1759-1764.
13. Nancollas GH, Zawacki SJ (1989). Calcium phosphate mineralization. *Connect Tissue Res* **21**: 239-246.
14. Nime FA, Hutchins G (1973). Oxalosis caused by *aspergillus* infection. *Johns Hopkins Med J* **133**: 183-194.
15. Philip LC (1972). *Microbiology*. WB Saunders, Philadelphia. pp. 293-295.
16. Pritzker KPH, Cheng PT, Grynepas MD, Holmyard DP (1988). Crystal associated diseases role of scanning electron microscopy in diagnosis. *Scanning Microsc* **2**: 1471-1478.
17. Romett JL, Newman RK (1982). Aspergillosis of the nose and paranasal sinus. *Laryngoscope* **92**: 764-766.
18. Schubert MM, Peterson DE, Meyers JD, Hackman R, Thomas ED (1986). Head and neck aspergillosis in patients undergoing bone marrow transplantation. Report of four cases and review of the literature. *Cancer* **57**: 1092-1096.
19. Shannon MT, Sclaroff A, Colm SJ (1990). Invasive aspergillosis of the maxilla in an immunocompromised patient. *Oral Surg Oral Med Oral Pathol* **70**: 425-427.
20. Tokunaga M, Tokunaga J, Harada K (1973). Scanning and transmission electron microscopy of sterigma and conidiospore formation in *aspergillus* group. *J Electron Microscopy* **22**: 27-38.

Discussion with Reviewers

A.L. Boskey: How do the authors know the material in the deposit is not debris generated by the extraction?

Authors: It is suggested that the calcium phosphate had been deposited in the fungus balls before the extraction. The likelihood of artificial deposition of calcium phosphate is remote, because the materials used for EDS and X-ray microdiffraction were washed with distilled water. Furthermore, the extracted material did not include bone

or tooth-like material macroscopically.

G. Daculsi: The identification of calcium phosphate is evident with EDS, but the demonstration of apatite, like biological apatite, in X-ray is unacceptable. The diagram revealed only poorly crystallized material, like amorphous calcium phosphate.

Authors: The X-ray microdiffraction diagram (Fig. 9) shows broader peaks even though using highly crystalline material. The position of the obtained peak maxima suggest the possibility of biological apatite, though we cannot deny the presence of poorly crystalline materials of other forms. However, we can compare our pattern to that of sialolith [Fig. 7A in reference 21].

G. Daculsi: The FT-IR data interpretation is incomplete. It is necessary to discuss the large difference between HAP and fungus balls (range 1400-1700, 800, 1200, 2950...).

Authors: The purpose of the FT-IR investigation in the present study was to discriminate between phosphate and oxalate in the fungus balls. The absorption bands at 565, 603, 872, 962 cm^{-1} corresponded to phosphate.

G. Daculsi: How do you explain the high sulfur content?

Authors: Sulfur is probably present as sulfated proteoglycans. These proteoglycans may have some function in the formation of pathological mineral.

G. Daculsi: Why, in this case, do you insist on comparison to HAP? The use of "calcium phosphate", rather than apatite, is enough!

Authors: We reported here that the calcified material deposited in a case of aspergillosis was calcium phosphate, not calcium oxalate.

G. Daculsi: How do you explain the high Ca/P ratio for a "biological apatite" ?

K.P.H. Pritzker: It is noted that the Ca/P ratio at 1.78 demonstrates excess calcium over that expected for Ca/P ratio in apatite 1.67. Has this excess calcium been deposited amorphously or in crystals? Can the authors determine this from their studies?

G. Valdre: The Ca/P molar ratio of fungus balls (1.78) is quite far from 1.67 of stoichiometric apatite. Could you comment on that? In addition, what is the role of Mg (3%)?

Authors: The Ca/P molar ratio of 1.78 for the fungus ball is considered to be due to crystalline biological apatite including carbonate, and the chemical composition may have shifted from phosphate to carbonate. We think that Mg may play an important role in the initial formation of biological apatite.

K.P.H. Pritzker: The authors seek to demonstrate apatite like calcium phosphate deposition in a case of maxillary sinus aspergillosis. This calcification is stated to occur in a necrotic area of fungi. What are the authors' criteria for necrotic fungi?

Authors: It is considered that the structures of *Aspergillus* are not observed inside the fungus balls by microscopy. Because *Aspergillus* is an aerobic fungus, it shows poor viability inside the fungus balls.

K.P.H. Pritzker: Figure 6 shows a crystal that does not have a habit associated with calcium apatite. It is possible that this structure is a calcium oxalate. Figure 7 shows a scanning electron micrograph which is consistent with calcium phosphate aggregates.

Authors: Figure 6 is not like the calcium oxalate structure that we have previously shown [Fig. 3 in reference 21].

Additional References

21. Yamamoto H, Sakae T, Takagi M, Otake S (1984). Scanning electron microscopic and X-ray microdiffractometric studies on sialolith-crystals in human submandibular glands. *Acta Pathol Jpn* 34: 47-53.